A Multiloop Robust Controller Design Study Using Singular Value Gradients

Jerry R. Newsom*
NASA Langley Research Center, Hampton, Virginia
and
V. Mukhopadhyay†
George Washington University
Joint Institute for Advancement of Flight Sciences, Hampton, Virginia

A method for designing robust feedback controllers for multiloop systems is presented. Robustness is characterized in terms of the minimum singular value of the system return difference matrix at the plant input. Analytical gradients of the singular values with respect to design variables in the controller are derived. A cumulative measure of the singular values and their gradients with respect to the design variables are used with a numerical optimization technique to increase the system's robustness. Both unconstrained and constrained optimization techniques are evaluated. Numerical results are presented for a two-input/two-output drone flight control system.

Nomenclature

A,B,C,D	= controller matrices
$\bar{A},\bar{B},\bar{C}$	= augmented system matrices
F,G_u,H	= plant matrices
G	= plant transfer matrix
g	= cumulative constraint
I	= identity matrix
$[I+KG]$	= return difference matrix
J	= objective function
j	$=\sqrt{-1}$
K	= controller transfer matrix
k_n	= nth loop gain perturbation in L matrix
L	= diagonal gain and phase change matrix
M	= order of controller
N_s,N_c,N_o	= order of plant, input, and output, respectively
p	= element of controller matrices
r	= reference input
s	= Laplace variable
u	= plant input vector
u_n,v_n	= left and right singular vectors
x	= plant state vector
x_c	= controller state vector
z	= plant output vector
β	= sideslip angle, deg
δ_1,δ_2	= elevon and rudder deflections, deg
σ_n	= nth singular value
$\bar{\sigma},\underline{\sigma}$	= maximum and minimum singular values
$\underline{\sigma}_M,\underline{\sigma}_D$	= global minimum and desired singular values
ϕ_n	= nth loop phase perturbation in L matrix
$\phi,\dot{\phi}$	= roll angle and rate, deg/s
$\psi,\dot{\psi}$	= yaw angle and rate, deg/s
ω	= frequency, rad/s
$[\ ]^*$	= complex conjugate transpose of $[\ ]$
$(\dot{})$	= represents time derivative of $(\ )$
$\mathrm{tr}[\ ]$	= trace of a square matrix $[\ ]$

Presented as Paper 83-2191 at the AIAA Guidance and Control Conference, Gatlinburg, Tenn., Aug. 15-17, 1983; submitted Sept. 9, 1983; revision received Oct. 22, 1984.

*Aerospace Engineer, Aeroservoelasticity Branch, Loads and Aeroelasticity Division. Member AIAA.
†Associate Research Professor. Senior Member AIAA.

Introduction

A WELL-DESIGNED feedback control system should provide stability robustness with respect to plant uncertainty. For single-input/single-output systems, the classical concepts of gain and phase margins are employed as measures of system robustness. In multiloop systems, these classical single-loop measures may not always provide a good measure of system robustness. Recently, matrix singular value properties of a multiloop system's return difference matrix have been proposed as a measure of system robustness.[1-4] Several authors have even related the singular values of the return difference matrix to multiloop gain and phase margins.[3,4]

The majority of the effort to date has focused on singular values as analysis tools. Only a small amount of effort has been focused on the use of singular values for control law synthesis.[5-7] Stein[5] discusses the frequency domain interpretation of the design based on the linear quadratic Gaussian (LQG) in terms of singular values. He shows how the LQG methodology can be used to design feedback controllers that satisfy design requirements expressed as singular value conditions. Safonov and Chen[7] discuss a procedure for maximizing singular values for stability margin optimization. The purpose of this paper is to introduce a new design method employing a numerical optimization technique to search for the controller design variables that increase the minimum singular value of the system return difference matrix. The singular value gradients required in the optimization schemes are derived analytically. Numerical results are computed for a two-input/two-output system that represents an experimental drone aircraft with a lateral attitude control system.[8]

System Description

Let the multiloop feedback system shown in Fig. 1 be decribed by a set of constant coefficient differential equations of the form

Plant:

$$\dot{x}=Fx+G_u u \tag{1}$$

$$z=Hx \tag{2}$$

Controller:

$$\dot{x}_c=Ax_c+Bz \tag{3}$$

$$u=Cx_c+Dz \tag{4}$$

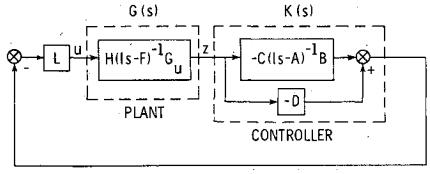

Fig. 1 Block diagram of a multiloop system.

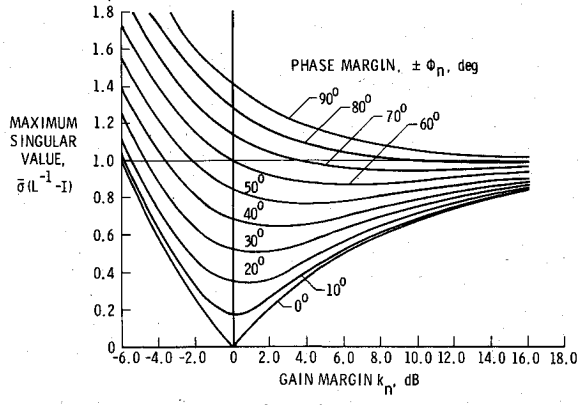

Fig. 2 Universal diagram for gain-phase margin evaluation.

Equation (1) represents an N_s order plant having N_o output measurements z, modeled by Eq. (2), and N_c control inputs u. Equations (3) and (4) represent an M-order feedback controller driven by the sensor output z. In terms of a transfer function matrix, the plant and the controller are

$$z=[H(Is-F)^{-1}G_u]u\equiv G(s)u \tag{5}$$

$$u=[C(Is-A)^{-1}B+D]z\equiv -K(s)z \tag{6}$$

respectively.

Assuming the closed-loop system to be stable and certain basic conditions (see Ref. 3), the robustness of the nominal system at the plant input can be examined by computing $\underline{\sigma}(I+KG)$ as a function of frequency ($s=j\omega$) and using the guaranteed stability criterion

$$\bar{\sigma}(L^{-1}-I)<\underline{\sigma}_M\leq\underline{\sigma}(I+KG)\qquad \underline{\sigma}_M\leq 1 \tag{7}$$

at all frequencies. In this paper, the matrix L is a diagonal gain and phase change matrix at the input of the plant as shown in Fig. 1,

$$L=\text{Diag}[k_n e^{j\phi_n}]$$

The matrix L is the identity matrix for the nominal system. It can be shown that

$$\bar{\sigma}(L^{-1}-I)=\max_n\sqrt{(1-1/k_n)^2+2(1-\cos\phi_n)/k_n}$$

$$n=1,2,\ldots N_c \tag{8}$$

Equation (8) is plotted in Fig. 2 (see Ref. 4 for details) with k_n and ϕ_n as parameters. This figure can be used to determine the guaranteed gain margins for a particular phase margin for simultaneous changes of both gain and phase in all input channels.[4]

It is widely known that singular values can be conservative estimates of robustness. A nonconservative measure of stability robustness directly applicable to uncertainty of the form L has been introduced in Ref. 13.

Singular Value Gradient Derivation

In order to perform the optimization, it is necessary to determine the gradients of the singular value $\underline{\sigma}(I+KG)$ with respect to elements in the controller quadruple matrices $A,B,C,$ and D. Let the parameter p represent one of the elements of the controller matrices. (These are the design variables.) It was shown in Ref. 4 that, for a distinct singular value σ_n of a complex matrix $(I+KG)$, the gradient with respect to a real parameter p is given by

$$\frac{\partial\sigma_n(I+KG)}{\partial p}=Re\left[u_n^*\frac{\partial(I+KG)}{\partial p}v_n\right] \tag{9}$$

where v_n and u_n are respectively right and left normalized singular vectors of $(I+KG)$. (For repeated singular values see Ref. 9 for the corresponding "Gateaux differential" expressions.)

It can be shown that

$$\frac{\partial\sigma_n(I+KG)}{\partial\hat{P}^T}=$$

$$Re[\hat{H}(Is-\bar{A})^{-1}\bar{B}(v_nu_n^*)[-I\,|\,\bar{C}(Is-\bar{A})^{-1}\bar{I}]]_{(N_o+M)\times(N_c+M)} \tag{10}$$

where

$$\hat{P}=\left[\begin{array}{c|c}D & C\\\hline B & A\end{array}\right]_{(N_c+M)\times(N_o+M)}$$

$$\hat{H}=\left[\begin{array}{c|c}H & 0\\\hline 0 & I\end{array}\right]_{(N_o+M)\times(N_s+M)}$$

$$\bar{A}=\left[\begin{array}{c|c}F & 0\\\hline BH & A\end{array}\right]_{(N_s+M)\times(N_s+M)}\qquad \bar{B}=\left[\begin{array}{c}G_u\\\hline 0\end{array}\right]_{(N_s+M)\times N_c}$$

$$\bar{C}=[-DH\,|\,-C]_{N_c\times(N_s+M)}\qquad \bar{I}=\left[\begin{array}{c}0\\\hline I\end{array}\right]_{(N_s+M)\times M}$$

To derive the matrix equation (10), define p as an element of the matrix $\hat{P}$. Then the scalar equation (9) can be written as

$$\frac{\partial\sigma_n(I+KG)}{\partial p}=Re\cdot\text{tr}\left[\frac{\partial(I+\bar{C}\Phi\bar{B})}{\partial p}v_nu_n^*\right]$$

$$=Re\cdot\text{tr}\left[\left\{\frac{\partial\bar{C}}{\partial p}\Phi\bar{B}+\bar{C}\Phi\frac{\partial\bar{B}}{\partial p}+\bar{C}\Phi\frac{\partial\bar{A}}{\partial p}\Phi\bar{B}\right\}v_nu_n^*\right] \tag{11}$$

where $\Phi=(Is-\bar{A})^{-1}$. Note that

$$\frac{\partial\bar{B}}{\partial p}=0$$

and

$$\bar{C}=\hat{I}_1\hat{P}\hat{H},\qquad \bar{A}=\hat{F}+\hat{I}_2\hat{P}\hat{H} \tag{12}$$

where

$$\hat{I}_1=[-I\,|\,0]_{N_c\times(N_c+M)}\qquad \hat{I}_2=\left[\begin{array}{c|c}0 & 0\\\hline 0 & I\end{array}\right]_{(N_s+M)\times(N_c+M)}$$

$$\hat{F}=\left[\begin{array}{c|c}F & 0\\\hline 0 & 0\end{array}\right]_{(N_s+M)\times(N_s+M)}$$

Equation (11) can be written as

$$\frac{\partial\sigma_n(I+KG)}{\partial p}=Re\cdot\text{tr}\left[\left\{\frac{\partial(\hat{I}_1\hat{P})}{\partial p}+\bar{C}\Phi\frac{\partial(\hat{I}_2\hat{P})}{\partial p}\right\}\hat{H}\Phi\bar{B}v_nu_n^*\right] \tag{13}$$

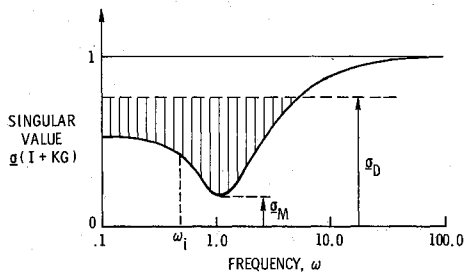

Fig. 3 Geometric description of cumulative objective function and cumulative constraints.

Using the matrix trace properties $Re\cdot\mathrm{tr}(A)=Re\cdot\mathrm{tr}(A^*)$, a matrix relation for the gradients with respect to all of the elements of $\hat{P}$ can be written as

$$\frac{\partial\sigma_n(I+KG)}{\partial\hat{P}}$$

$$=Re[\{\hat{I}_I^T+(\bar{C}\Phi\hat{I}_2)^*\}\{\hat{H}\Phi\bar{B}v_n u_n^*\}^*]_{(N_c+M)\times(N_o+M)} \quad (14)$$

The complex conjugate transpose of Eq. (14) gives Eq. (10). The gradient expressions for the matrices $(I+KG)^{-1}$, KG, $KG(I+KG)^{-1}$ can be obtained in the same manner and are given in the Appendix. Two additional computations are involved in computing singular value gradients at each frequency point. The first computation is the solution of a set of (N_s+M) simultaneous equations and is relatively inexpensive since the matrix A is already available in upper Hessenberg form[10] from the computation of the singular values. The second is the computation of the singular vectors and generally involves a low-order complex matrix.

Optimization Schemes

Let us assume that the minimum over the frequency domain of the singular value $\underline{\sigma}(I+KG)$ of a stable system is $\underline{\sigma}_M$. It is desired to increase $\underline{\sigma}_M$ to a desired value $\underline{\sigma}_D$ as illustrated in Fig. 3. An increased $\underline{\sigma}_M$ results in better gain and phase margins of the system, as is shown in Eq. (7) and Fig. 2. Optimization schemes to achieve this objective using the gradient information of Eq. (10) are described next.

The selection of an achievable $\underline{\sigma}_D$ is based on engineering judgment consistent with control system limitations, since control effort might be wasted in designing a compensator to satisfy Eq. (7) with an arbitrarily high $\underline{\sigma}_D$. Moreover, due to the conservative nature of singular value measures, inability to obtain such a compensator does not necessarily imply a robustness problem.

Unconstrained Minimization Approach

In the unconstrained minimization approach, a single objective function J is minimized by changing the design variables p. Since $\underline{\sigma}(I+KG)$ is less than $\underline{\sigma}_D$ over a range of frequencies instead of at a single point, all of the violations where $\underline{\sigma}(I+KG)<\underline{\sigma}_D$ are represented by a single cumulative measure $J(p)$

$$J(p)=\sum_i(\mathrm{Max}\{0,[\underline{\sigma}_D-\underline{\sigma}(j\omega_i,p)]\})^2 \quad (15)$$

The summation is taken over a large number of frequency points where both the choice of the frequency range and spacing of the frequency points in a frequency range are left to the designer. A geometric description of the cumulative objective function is shown in Fig. 3. The objective is to minimize (preferably reduce to zero) the shaded area below the $\underline{\sigma}_D$ line. A conjugate gradient algorithm[11] is used to search for the controller design variables p that minimize J without allowing $\underline{\sigma}$ to go near zero during the search process. Not allowing $\underline{\sigma}$ to go near zero is particularly important to avoid destabilizing the system during the linear search process, especially when $\underline{\sigma}$ has sharp drops at specific frequencies. The method is expected to work when $\underline{\sigma}$ and $\partial\underline{\sigma}/\partial p$ variations with frequency are not too large over small frequency ranges. If J can be reduced to zero, then the minimum singular value reaches $\underline{\sigma}_D$ or higher.

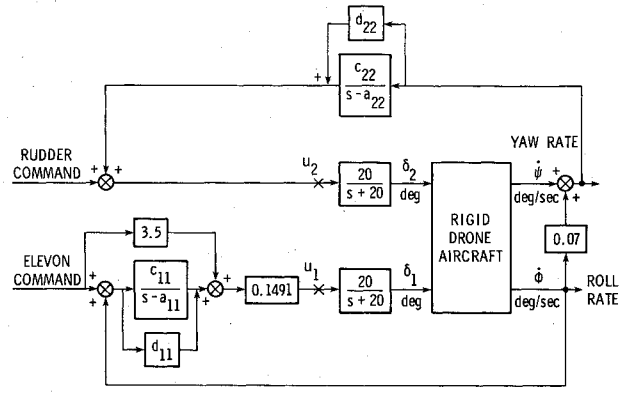

Fig. 4 Block diagram of a drone lateral attitude control system.

Constrained Minimization Approach

In the constrained minimization approach, an objective function J is minimized with respect to the design variables p, subject to the inequality constraint $g\leq 0$. In this approach, the cumulative measure of all of the violations $\underline{\sigma}(I+KG)<\underline{\sigma}_D$ is treated as the constraint.[12] The objective function J and the constraint g are defined as

$$J(p)=\tfrac{1}{2}\mathrm{tr}[C^TC] \quad (16)$$

$$g(p)=\sum_i(\mathrm{Max}\{0,[\underline{\sigma}_D-\underline{\sigma}(j\omega_i,p)]\})^2 \quad (17)$$

The choice of J in Eq. (16) is desirable since a lower C is reflected in lower control activity. Other choices of J are possible. In Eq. (17), the summation is taken over a large number of frequency points as before. A geometric description of the cumulative constraint is shown in Fig. 3. The objective is to reduce the shaded area to zero by satisfying the inequality constraint $g\leq 0$. Although the present paper is confined to a single constraint, additional constraints on responses and singular value bounds at other points in the loop can be considered for an overall design. The method of feasible directions[11] is used to search for the controller design variables p that minimize J subject to $g\leq 0$. The method uses the objective function and constraint gradient information to determine a parameter move direction and a scalar multiplier in the usable-feasible direction to satisfy all constraints. When the constraint condition is satisfied, then $g\leq 0$, which implies $\underline{\sigma}\geq\underline{\sigma}_D$ for all ω_i from the definition of g in Eq. (17).

Numerical Results

Numerical results are presented for a two-input/two-output system representing a drone aircraft with a lateral attitude control system.[4,8] A nominal controller is available for comparison. The present method is used to increase the robustness by redesigning the nominal controller. A block diagram of the drone lateral attitude control system is shown in Fig. 4.[8] The plant state vector x is defined as

$$x=\lfloor\beta\ \dot{\phi}\ \dot{\psi}\ \phi\ \delta_1/20\ \delta_2/20\rfloor^T$$

The plant matrices F, G_u, and H as defined in Eqs. (1) and (2) and the nominal controller matrices A,B,C, and D as defined in Eqs. (3) and (4) are given in Ref. 4. The eigenvalues of the nominal open- and closed-loop systems are given in Table 1. The eigenvalue at $\lambda=0.1889\pm j1.051$ results in an unstable

Table 1 Eigenvalues of drone lateral attitude control system

Mode	Open loop	Closed loop		
		Nominal	Design 1	Design 2
1	−0.03701	−0.6911	−0.0386	−0.01399
2,3	$0.1889 \pm j1.051$	$-0.2553 \pm j1.187$	$-0.6436 \pm j0.823$	$-0.5336 \pm j0.959$
4	−3.25	−2.60	$-6.225 \pm j2.342$	$-3.866 \pm j2.276$
5	−20.0	−18.70	−11.11	−16.08
6	−20.0	−20.15	−20.02	−20.00
7		0	0	0
8		−2.261		

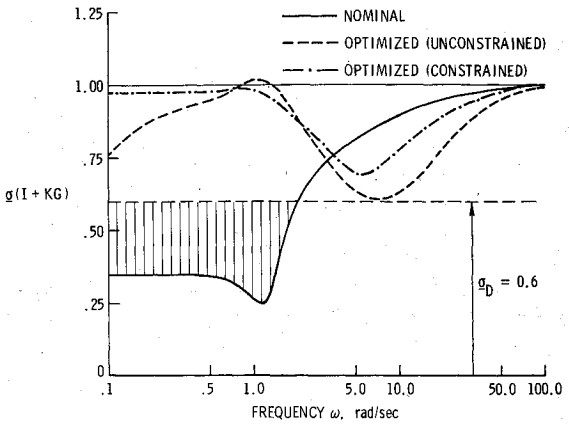

Fig. 5 Minimum singular value vs frequency plot for nominal and optimized control laws.

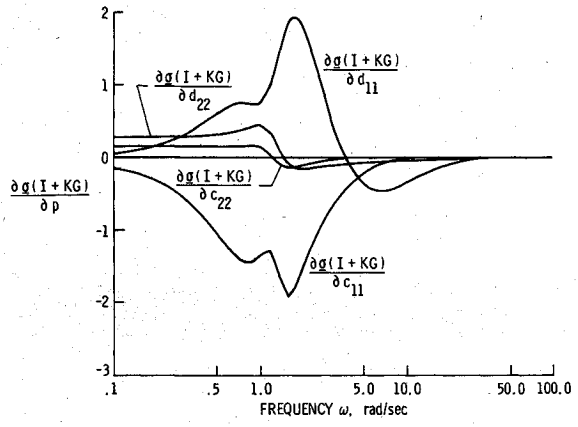

Fig. 6a Gradient of singular value $\underline{\sigma}(I+KG)$ with respect to controller parameters a_{11}, a_{22}, b_{11}, and b_{22} (nominal).

dutch-roll mode. The elements of the input vector are the elevon and rudder actuator commands, reespectively. All gain and phase changes are considered at the points X in Fig. 4. The minimum singular value of the return difference matrix $(I+KG)$ over the operating frequency range is plotted in Fig. 5 for the nominal system. The minimum singular value is constant at 0.35 over low frequencies, then drops to its lowest value of 0.25 near 1.2 rad/s, which is close to the frequency of the unstable open-loop pole. The minimum singular value approaches unity asymptotically as KG attenuates at higher frequencies. Using the stability condition given in Eq. (7), the stability is guaranteed if $\bar{\sigma}(L^{-1}-I)<0.25$. This can be interpreted in terms of gain and phase margins using Fig. 2. The guaranteed simultaneous gain margins are −2.0 and 2.5 dB ($\phi_1=\phi_2=0$). The simultaneous phase margins are ±15 deg ($k_1=k_2=0$ dB).

Figures 6a and 6b show the gradients of $\underline{\sigma}(I+KG)$ with respect to the nominal controller parameters $a_{11}, a_{22}, \ldots, d_{22}$. The locations of these parameters in the block diagram are shown in Fig. 4. The elements b_{11} and b_{22} do not appear in Fig. 4 since their unity values are embedded in the controller structure. The gradients with respect to c_{11} and d_{11} are quite large. The gradients with respect to other diagonal elements a_{11}, a_{22}, c_{22}, d_{22}, etc., are relatively small. These gradients attenuate to zero before 10 rad/s except for the one with respect to d_{11}, which attenuates at 30 rad/s. It may be noted that, although the off-diagonal elements are zero, the singular value gradients with respect to them are quite large.

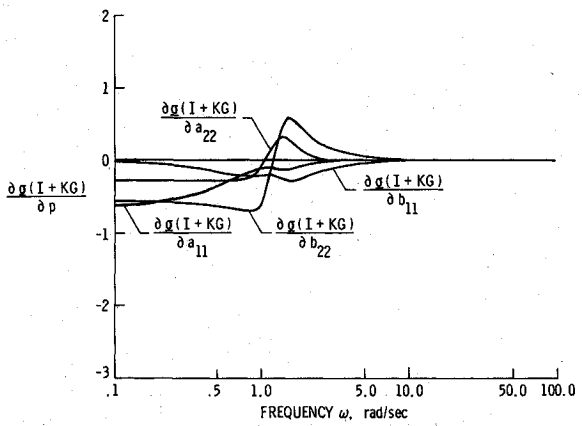

Fig. 6b Gradient of singular value $\underline{\sigma}(I+KG)$ with respect to controller parameters c_{11}, c_{22}, d_{11}, and d_{22} (nominal).

Results of Unconstrained Minimization (Design 1)

Unconstrained minimization is performed using c_{11} and d_{22} as the design parameters. The desired minimum singular value $\underline{\sigma}_D$ is 0.6. The equality relations $d_{11}=0$ and $c_{22}=a_{22}d_{22}$ are maintained to satisfy the $1/s$ and $s/(s+2)$ structure of the nominal control law. Hence, the design parameters are basically proportional to gains in each loop. Although the convergence patterns of both the objective function and the design variables are not shown, the objective function reduces to zero in one iteration and the values of c_{11} and d_{22} are 0.13

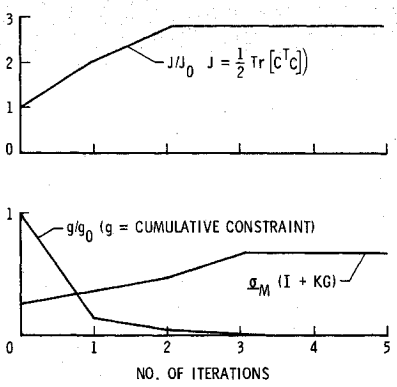

Fig. 7 Convergence pattern of constrained minimization (design 2).

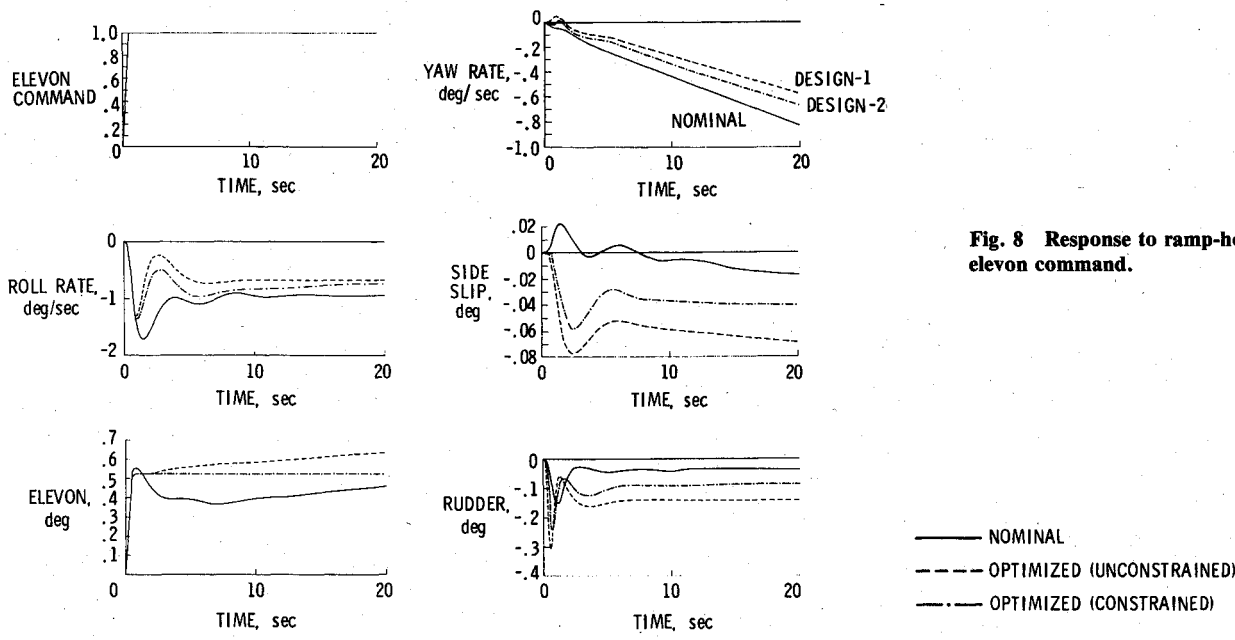

Fig. 8 Response to ramp-hold elevon command.

and 9.69, respectively. Note that $c_{22} = -2d_{22} = -19.38$. The singular value plot is shown in Fig. 5 as design 1. The minimum singular value $\underline{\sigma}_M$ is 0.6 as desired. The price paid for the higher value of $\underline{\sigma}_M$ is the loss of rapid attenuation at higher frequencies. When $\underline{\sigma}_M = 0.6$, the guaranteed gain margins are -4.1 and 8.0 dB and the phase margins are ± 35 deg. This reflects substantial improvement over the nominal stability margins. The eigenvalues of the closed-loop system are given in Table 1.

Results of Constrained Minimization (Design 2)

Next, the same problem is solved using the constrained optimization approach defined as design 2. The desired minimum singular value $\underline{\sigma}_D$ is again 0.6. The objective function is chosen as defined by Eq. (16). The convergence pattern for design 2 is shown in Fig. 7. The J and g are normalized by their starting value J_0 and g_0, respectively. The constraint is satisfied in three iterations, but at the cost of increased J. The values of c_{11} and d_{22} after five iterations are 2.08×10^{-6} and 5.91, respectively. The corresponding singular value plot is shown in Fig. 5 as design 2. The minimum singular value $\underline{\sigma}_M = 0.68$. The loss of attenuation at higher frequencies is much less as compared to design 1, probably because the algorithm tries to minimize the growth of $0.5(c_{11}^2 + c_{22}^2)$ as well. The eigenvalues of the closed-loop system are given in Table 1.

As a general rule, an increase in robustness is accompanied by degraded response and increased control activity. This effect is examined from time-response plots of the closed-loop system using the nominal, design 1, and design 2 controllers presented in Fig. 8. The input is a unit ramp-hold elevon command that rises linearly from 0 to 1 in 0.4 s. The increases in sideslip from the nominal are roughly four times for design 1 and twice for design 2. The roll and yaw rates are 10-20% lower than nominal. The elevon activity increases by 25% for design 1 and 10% for design 2. The increase in rudder activity is roughly three times for design 1 and twice for design 2 with large initial overshoot.

Conclusions

A method for designing feedback controllers to increase the robustness of multiloop systems has been presented. Gradients of the singular values of the return difference matrix with respect to design variables in the controller were derived analytically. A cumulative measure of the singular values and their gradients was used with a numerical optimization algorithm to increase the system's robustness.

A numerical example was given to illustrate the method. For the example, a nominal controller was available. The present method was used to design a new controller that provided increased robustness. The global minimum singular value was increased substantially using both the unconstrained optimization approach and the constrained optimization approach. For both of these cases, the time response of the system using these controllers was degraded. Some high-frequency attenuation was lost. For a better overall design, more constraints need to be added and further development is necessary.

Appendix

The singular value gradients of some useful matrices with respect to the controller quadruple $\hat{P}$ is presented below. The left and right singular vectors u_n and v_n in each expression belong to the singular value of that particular matrix.

$$\frac{\sigma_n(I+KG)^{-1}}{\partial \hat{P}^T} = -Re[\hat{H}\Phi_a \bar{B} v_n u_n^* [-(I+KG)^{-1} \bar{C}\Phi_a \bar{I}]]$$

$$\frac{\partial \sigma_n(KG)}{\partial \hat{P}^T} = Re[\hat{H}\Phi \bar{B} v_n u_n^* [-I \bar{C}\Phi \bar{I}]]$$

$$\frac{\partial \sigma_n(KG(I+KG)^{-1})}{\partial \hat{P}^T} = Re[\hat{H}\Phi_a \bar{B} v_n u_n^* [-(I+KG)^{-1} \bar{C}\Phi_a \bar{I}]]$$

where

$$\Phi_a = (Is - \bar{A} + \bar{B}\bar{C})^{-1}$$

The gradient expression for $\underline{\sigma}(GK)$, etc., at the output can be derived similarly starting from Eq. (9).

References

[1]Safonov, M.G., Laub, A.J., and Hartmann, G.L., "Feedback Properties of Multivariable Systems: The Role and Use of the Return Difference Matrix," *IEEE Transactions on Automatic Control,* Vol. AC-26, No. 1, Feb. 1981, pp. 47-65.

[2]Doyle, J.C. and Stein, G., "Multivariable Feedback Design: Concepts for a Classical/Modern Synthesis," *IEEE Transactions on Automatic Control,* Vol. AC-26, No. 1, Feb. 1981, pp. 4-16.

[3]Lehtomaki, N.A., Sandell, N.S. Jr., and Athans, M., "Robustness Results in Linear Quadratic Gaussian Based Multivariable Control Designs," *IEEE Transactions on Automatic Control,* Vol. 26, No. 1, Feb. 1981, pp. 75-92.

[4]Mukhopadhyay, V. and Newsom, J.R., "A Multiloop System Stability Margin Study Using Matrix Singular Values," *Journal of Guidance, Control, and Dynamics,* Vol. 7, Sept.-Oct. 1984, pp. 582-587.

[5]Stein, G., "LQG-Based Multivariable Design: Frequency Domain Interpretation," *Multivariable Analysis and Design Techniques,* AGARD Lecture Series 117, Sept. 1981, pp. 5.1-5.9.

[6]Doyle, J.C., "Multivariable Design Techniques Based on Singular Value Generalizations of Classical Control," *Multivariable Analysis and Design Techniques,* AGARD Lecture Series 117, Sept. 1981, pp. 4.1-4.9.

[7]Safonov, M.G. and Chen, B.S., "Multi-variable Stability-Margin Optimization With Decoupling and Output Regulation," *Proceedings of the IEE,* Vol. 129, Pt. D., No. 6, Nov. 1982, pp. 276-282.

[8]Perry, B., "Methodology for Determining Elevon Deflections to Trim and Maneuver the DAST Vehicle with Negative Static Margin," NASA TM-84499, May 1982.

[9]Freudenberg, J.S., Looze, D.P., and Cruz, J.B., "Robustness Analysis Using Singular Value Sensitivities," *International Journal of Control,* Vol. 35, No. 1, 1982, pp. 95-116.

[10]Laub, A.J., "Efficient Multivariable Frequency Response Computations," *IEEE Transactions on Automatic Control,* Vol. AC-26, No. 2, April 1981, pp. 407-408.

[11]Vanderplaats, G.N., "CONMIN-A FORTRAN Program for Constrained Function Minimization-User Manual," NASA TM X-62282, Aug. 1973.

[12]Greene, W.H. and Sobieszczanski-Sobieski, J., "Minimum Mass Sizing of a Large Low-Aspect Ratio Airframe for Flutter-Free Performance," *Journal of Aircraft,* Vol. 19, March 1982, pp. 228-234.

[13]Doyle, J.C., Wall, J.E., and Stein, G., "Performance and Robustness Analysis for Structured Uncertainty," *Proceedings of the 1982 IEEE Conference on Decision and Control,* Dec. 1982, pp. 629-636.